



Hannibal ad portas: predicting the potential distribution of the exotic wood decay fungus *Coniophora olivacea*, new in Patagonia

Hannibal ad portas: prediciendo la distribución potencial del hongo exótico degradador de madera *Coniophora olivacea*, nuevo en Patagonia

Fernando Moro Cordobés¹; Paola Almonacid²; Oscar Troncoso²; Gonzalo Romano³; Francisco Kuhar^{1,4*}

¹ Innomy Biotech, Astondo bidea, Building N° 612 Bizkaia Technology Park, (48160) Derio, País Vasco.

² Universidad Nacional de la Patagonia San Juan Bosco, Ruta 259, Km 16,4, (9200) Esquel, Chubut, Argentina.

³ Fundación Hongos de Argentina para la Sustentabilidad. Molinari 1657, (9200) Esquel, Chubut, Argentina.

⁴ Instituto Interdisciplinario de Biología Vegetal (CONICET – UNC), Casilla de Correo 495, (5000) Córdoba, Argentina.

* Corresponding author: <fkuhar@gmail.com>

ABSTRACT

Coniophora olivacea has been traditionally considered as an important decay agent of building timbers of broadleaf and conifer woods, and causes significant damage on doors, window frames and other wood structures exposed to the environment. A more restricted role as tree pathogen has been also reported in cold climates. Studies of the predicted distribution of potentially invasive species are a useful tool to focus management efforts. Maximum-Entropy models allow predictions based on climatic and altitudinal layers as well as on previous data on the occurrence of species. The aim of this work is to report the presence of this wood decay fungus for the first time in Patagonia, and also to predict the potential spread pattern of this species using Maximum-Entropy.

Keywords — Maxent; biological invasion; brown rot; *Nothofagus*.

► Ref. bibliográfica: Moro Cordobés, F.; Almonacid, P.; Troncoso, O.; Romano, G.; Kuhar, F. 2023. *Hannibal ad portas*: predicting the potential distribution of the exotic wood decay fungus *Coniophora olivacea*, new in Patagonia. *Lilloa* 60 (2): 149-169. doi: <https://doi.org/10.30550/j.lil/1801>

► Recibido: 1 de junio 2022 – Aceptado: 3 de agosto 2023 – Publicado en línea: 22 de agosto 2023.



► URL de la revista: <http://lilloa.lillo.org.ar>

► Esta obra está bajo una Licencia Creative Commons Atribución – No Comercial – Sin Obra Derivada 4.0 Internacional.

RESUMEN

Coniophora olivacea se ha considerado tradicionalmente un importante degradador de madera en obra de coníferas y latifoliadas, y también se reportan daños en puertas, marcos de ventanas y otras estructuras de madera expuestas a la intemperie. Un rol más restringido como patógeno forestal se ha citado en climas fríos. Los estudios que predicen la distribución de especies potencialmente invasoras son una herramienta para focalizar los esfuerzos de manejo de las mismas. Los modelos de Máxima Entropía permiten predicciones basadas en capas altitudinales y climáticas, así como también en datos preexistentes sobre la distribución de las especies. El objetivo de este trabajo es reportar la presencia de este degradador por primera vez en Patagonia, y estudiar sus patrones de propagación usando modelos de Máxima Entropía orientados a predecir su comportamiento.

Palabras clave — Maxent; invasión biológica; pudrición castaña; *Nothofagus*.

INTRODUCTION

The genus *Coniophora* (Coniophoraceae, Boletales) is a widespread brown-rot wood decay fungus occurring in building timber as well as in natural environments, mostly in temperate regions (Kauserud et al., 2007). *Coniophora arida* and *C. olivacea* have been recorded on dead wood of diverse tree species, both conifer and hardwood timber, and are distributed in northern and southern temperate zones worldwide. *Coniophora olivacea* has also been reported on living *Picea* spp. in North America. Both *C. arida* and *C. olivacea* are common in coniferous forests (Ginns, 1982). Together with *C. puteana*, they cause economically important losses in several ways; they frequently cause decay of living trees and have been observed indoors on construction materials (Kauserud et al., 2007). Chee et al. (1998) report significant weight losses of wood in solid-state cultures of *C. olivacea*. Da Costa et al. (1967) also mention the capability of vigorous attack of this species on a very wide range of timbers under different uses, including hardwood trees such as *Eucalyptus marginata* in Western Australia. They also report that wood density was significantly affected by *Coniophora olivacea* whereas other fungal species tested did not significantly alter this parameter. Rudman (1963) proves that the sapwood of many tree species is uniformly susceptible to attack by this fungus. Although the infective role of each dissemination form is yet unknown (Edman & Jonsson, 2001), *C. olivacea* is able to produce basidiospores as well as mycelial cords (Stalpers, 1978), which suggests the possibility of infection through the soil from one log to another.

A specimen collected by the authors identified as *C. olivacea* and deposited at the CORD Herbarium (CORD FK16004) is to our knowledge the first and only record of this species in southern South America. Since the Andean Patagonia has a long history of cultivation of non-native trees species (e.g. *Pinus* spp., *Eucalyptus* spp., *Pseudotsuga menziesii*, among others), events of introduction of exotic fungal species are likely. Moreover, intense fieldwork performed in the last decades by many

mycologists aiming to assess in depth the aphyllorphoroid fungi of the region did not detect this species (e.g., Greslebin & Rajchenberg, 2003).

Our collection consists of a small decayed piece of wood found on soil in a mixed forest. Given the fragmentary nature of the material, the identity of the wood species of the substrate is not obvious, and intensive histochemical work is needed to accurately identify it.

Since *C. olivacea* has been shown to be capable of producing significant damage in wooden structures, reliable information is needed as a base for future management programs. Strategies aiming to restrict the dispersion of forest pathogens, such as *Phytophthora austrocedri*, have been already promoted (Giordana *et al.*, 2020), including restrictions in tourism and animal farming in certain areas or even chemical treatments (Silva *et al.*, 2016). Initiatives against the spread of *C. olivacea* as well as against other non-native species might be needed in the future, even if they do not mainly affect living trees, since wood is the dominant construction material in the region, especially in the Chilean slope of the Andes.

Given the complex and multicausal nature of biological invasions, it is difficult to predict the behavior of a newly arrived alien species in a given area is, at least, challenging (Desprez-Loustau *et al.*, 2007), especially when this behavior is also linked to plant species that might act as hosts, partners or reservoirs of the fungal entity (Dickie *et al.*, 2017). However, methods taking on account climatic and other variables produce robust models outlining the potential distribution of a species given their environmental preferences. In this line, Maximum Entropy (Maxent) models have been shown to be efficient in estimating the potential geographic distributions of species by merging presence-only data with environmental information (Phillips *et al.*, 2006; Yuan *et al.*, 2015).

An additional challenge regarding the identification of *C. olivacea* is the presence of distinct evolutionary clades within this species (Kausserud *et al.*, 2007). Since this diversity is morphologically cryptic, only molecular methodologies can place a specimen in this scheme. Studies taking into account this hidden diversity and aiming to find different behaviors (e.g. in degradation, dispersal, infectivity) need available material associated with reliable information on the specimen.

The aim of this work is to provide reliable information on the identity, host and potential distribution of *C. olivacea*, reported here as new for Patagonia, so future decisions on non-native species management can be made on a solid basis.

MATERIALS AND METHODS

Sequences and molecular analyses

DNA of the vouchered specimen was extracted with the GenElute Plant Genomic DNA Miniprep Kit (SigmaAldrich) following the manufacturer's instructions. The rDNA ITS1-5.8S-ITS2 region (ITS) was amplified using the primers ITS1F/ITS4 White *et al.*, 1990; Gardes & Bruns, 1993). The PCR reaction was performed with the REDExtract-N-Amp PCR ReadyMix (SigmaAldrich) for both regions under the

following conditions: an initial denaturing step at 95 °C for 4 min, 36 cycles of 30 s at 94 °C, 45 s at 55 °C and 70 s at 72 °C and a final extension for 10 min at 72 °C. The amplified DNA fragment was purified and sequenced in Macrogen (Seoul, South Korea) using the primer ITS4 for ITS. This newly generated sequence was uploaded to GenBank with the accession number ON832657. Internal Transcribed Spacer sequences of the most similar taxa identified to species were queried in GenBank NCBI (<http://www.ncbi.nlm.gov>) using the MEGABLAST option (see Table S1). Sequences of specimens of the genus *Leucogyrophana* were recovered from GenBank and used to root the tree.

The sequences were aligned with L-INS-i strategy as implemented in MAFFT 7.0 (Kato & Standley, 2013) and analyzed without additional editing. Nucleotide substitution models were chosen with jModelTest 2.1 (Darriba *et al.*, 2012), under the Akaike information criterion (AIC). Maximum likelihood (ML) analysis was performed in PHYML (Guindon *et al.*, 2010). Bootstrap values of the most likely tree were calculated after 1,000 repetitions with 10 random addition sequences and the topologies were produced using TBR swapping. B/MCMC analyses were conducted with MrBayes (Huelsenbeck & Ronquist, 2001) with 7,000,000 generations starting with a random tree and running four simultaneous chains. The first 100,000 generations were discarded as burn-in. TRACER1 (<http://evolve.zoo.ox.ac.uk/software.html/tracer/>) was used to verify that stationarity was achieved after the first 100,000 generations.

Wood identification and characterization of the damage

Transverse, tangential and radial sections (10 μ m thick) were made using a Leica Hn 40 sledge microtome and stained with cotton blue, after bleaching the wood with hydrogen peroxide 30% for 1.30 h, rinsing with distilled water 3 to 4 times, and rinsing before mounting in lactoglycerol. Ten slides of each sample were mounted and 10 unstained slides were prepared as control. Observations were made under a light microscope Leica DM500 and photomicrographs were obtained with a Canon EOS Rebel T3i digital camera. Wood library samples and the InsideWood database (<http://insidewood.lib.ncsu.edu>) were used for comparative study and to determine the species identity of the wood substrate.

The slides (at least 5 for each section of the procedures of noninfected and infected wood) were stained using specific procedures mentioned by Krishnamurthy (1988) for localizing lignin, carbohydrates, and other phenolics. Lignin was revealed as red using Wiesner's reagent for five minutes and mounted on a drop of 6N HCl. Toluidine blue was used to contrast lignin and polyphenols (turquoise green), carbohydrates (lilac) and oils (without color), and rinsed with water (Rivera Nava *et al.*, 1999).

Occurrence data, climatic data, and niche modeling

Ecological niche model (ENM) was employed to infer the potential distribution of *C. olivacea* in the world, with a special focus on Patagonia. Geographical coordinates of curated registers of this species were recorded from Global Biodiversity Information Facility (GBIF website: www.gbif.org) and also from BLAST queries of ITS sequences in public databases included in the phylogenetic analyses (Table S2). Records before 1950 were eliminated since climatic data before is not systematically curated. Records without documented authoritative identification were also discarded. To avoid an autocorrelation spatial effect in the ENM, the points located closer than 50 km from each other were eliminated using the R package “Wallace” v1.0.6.1 (Kass *et al.*, 2018) implemented in R v3.6.1. The final database contained 113 records distributed on every continent except Antarctica (Table S2).

A set of 19 bioclimatic variables layers and one elevation layer were obtained from the WorldClim 2 database (<http://www.worldclim.org>) at 2.5 arc-min (i.e. ca. 5 km) resolution covering the entire planet (Hijmans *et al.*, 2005). In order to minimize biased fitting of the models produced by the covariance between variables, Pearson’s correlation was performed to eliminate correlated environmental and elevation variables using R v3.6.1. After we excluded correlated variables ($r > 0.7$), we selected six climatic variables (Fig. S1): Bio1 (annual mean temperature), Bio2 (mean diurnal range), Bio4 (annual temperature range), Bio11 (precipitation of driest month), Bio12 (annual precipitation), Bio15 (precipitation seasonality) and the elevation variable. MaxEnt was run under default settings, including auto-features, a maximum of 500 iterations, 100 replicates to ensure reliable results, and 10,000 randomly sampled background points, with a regularization multiplier of 1 and a convergence threshold of 10^{-5} . K-fold cross-validation was used to test the performance of the model. To do this, occurrence data were randomly split into a number of equal-size groups, and models are created after resampling the set. The left-out folds were then used for evaluation. Logistic output models were produced and uploaded to ASCII in raster format and then imported to the QGIS “Geographic Information System” Version 3.4.12 (2019). The average model was geographically projected dividing the probability of occurrence into five categories: values below the threshold were considered absent, “low” threshold–0.25, “medium” 0.25–0.5, “high” 0.5–0.75, and “very high” > 0.75 . The area under the “receiver operating characteristic (ROC) curve” (AUC) values (Peterson *et al.*, 2008; Elith & Leathwick, 2009) were used to evaluate the fitness of the prediction. Variable importance to ENMs was evaluated based on the permutation value, percent contribution, jackknife resampling, and the response curves produced by MaxEnt (Phillips *et al.*, 2017).

RESULTS

Molecular identification

The analyses performed to support the morphological identification of the voucher FK16004 as *Coniophora olivacea* (Fr.) P. Karst. (Fig. 1) and also strongly suggest that

this material is affiliated with group 4 within the scheme proposed by Kausrud *et al.* (2007). This group consists of materials found in British Columbia (Canada) and the UK, and Kausrud *et al.* (2007) conclude that this lineage probably has a wider boreal distribution. But more profound studies and a wider sampling is needed before proposing these localities as the origin of the introduced strain. Group 5 has not been recovered from the dataset since no available sequences representing it were retrieved from public databases.

Identification of the substrate and effect of the degradation

The woody substrate presented the following characteristics: In cross-section, diffuse porosity was observed, with solitary and grouped vessels colonized by abundant hyphae. Sectors without fibers or parenchymal rays (disintegrated tissue) were observed. In the radial section, rays of reddish coloration and with contents were

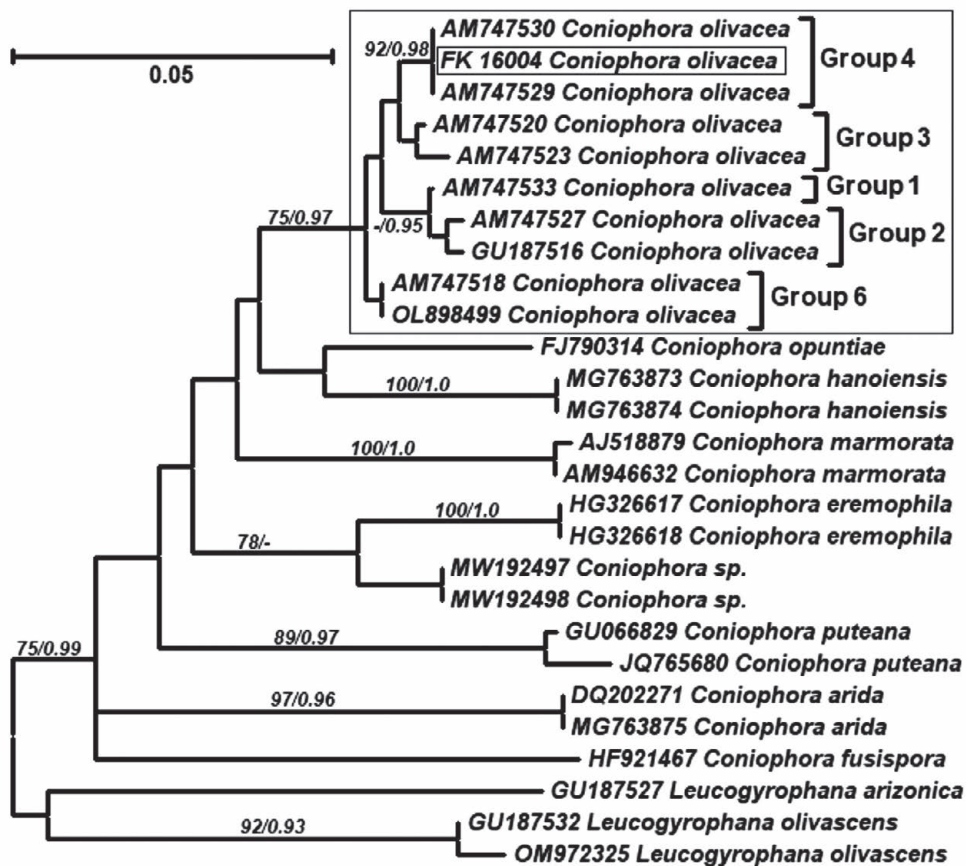


Fig. 1. Maximum likelihood tree showing significant bootstrap support (>75%) and significant Bayesian PP (>0.95). Intraspecific groups indicated in *C. olivacea* correspond to the cryptic clades defined by Kausrud *et al.* (2007). Group 5 was not recovered due to the lack of representative sequences.

Fig. 1. Árbol de Máxima verosimilitud con valores significativos de bootstrap (>75%) y PP Bayesianas (>0.95). Los grupos intraespecíficos indicados en *C. olivacea* corresponden a los clados crípticos definidos por Kausrud *et al.* (2007). El grupo 5 no está representado debido a la falta de secuencias.

observed as well as vessels with abundant hyphae. Tangential sections made evident that rays are almost exclusively uniseriate. Vessel elements with oblique septa and opposite, scalariform intervessel pits, and with a large number of hyphae were also observed. These anatomical characteristics are coincident with *Nothofagus dombeyi* (Mirb.) Oerst wood, which has diffuse porosity, solitary and grouped vessels, in radial, multiple, short and long series (Rivera, 1988). In tangential section, *N. dombeyi* presents oblique septa, and in radial section, simple perforation plates bordering each other, with subterminal, opposite (often scalariform) intervessel pits with circular to elliptical areolae. Rays are almost exclusively uniseriate, with procumbent cells (Tortorelli, 2009).

In transverse sections, the noninfected wood tested positive for lignin, where the fibers and rays are stained to a pink/red color (Fig. 2A), while in the wood colonized by *C. olivacea* no positive reaction to lignin was detected. The fibers showed thin and deformed walls, and some showed cellular contents. The rays showed other colors with some reddish contents (Fig. 2B). In tangential longitudinal sections of noninfected wood, the fibers and walls of the vessels were stained to reddish/pink, evincing the presence of lignin (Fig. 2C). The wood showed a brownish coloration as well as no positive reaction for lignin (Fig. 2D).

Fibers of native (noninfected) tissues in the cross-section showed lignin presence, as evinced by the blue color, indicative of this compound, whereas the rays showed a green coloration (a weaker reaction for the presence of lignin) with dark contents. The deposits in some vessels displayed a pink reaction indicating the presence of carbohydrates (Fig. 2E). In the tangential longitudinal section, the walls of the vessels showed intervessel pits stained with color blue as well as fibers, indicating the presence of lignin (Fig. 2G).

The cross-section of the infected wood showed fibers with thinner cell walls and rays with enlarged and ocher-colored contents that evince an advanced state of degradation. The vessels were observed to be translucent (white) due to the loss of carbohydrates and the absence of other contents (Fig. 2F). The situation was similar in the tangential section, where deformed vessels were also observed (Fig. 2H).

EMN of *C. olivacea* and potential distribution in Patagonia

The potential distribution model of *C. olivacea* exhibited a high predictive power, as shown by the AUC (μ : 0.902; SD: 0.114). The maps obtained from ENM showed how the habitat suitability is distributed globally (Fig. S3), including in the Patagonia region (Fig. 3). In general, suitable areas were located in Europe, North and South America, Australia, and East Asia. The model also predicted suitable areas in Argentina and Chile, which can represent geographic regions with an adequate combination of climatic and elevation conditions for the establishment of *C. olivacea* (Fig. 3). The areas with high suitability values (> 0.5), occupied approximately 629,053 km² of the total area of Argentina and Chile (Fig. 3). According to this model, the main variables explaining the presence of the species were Bio12 (annu-

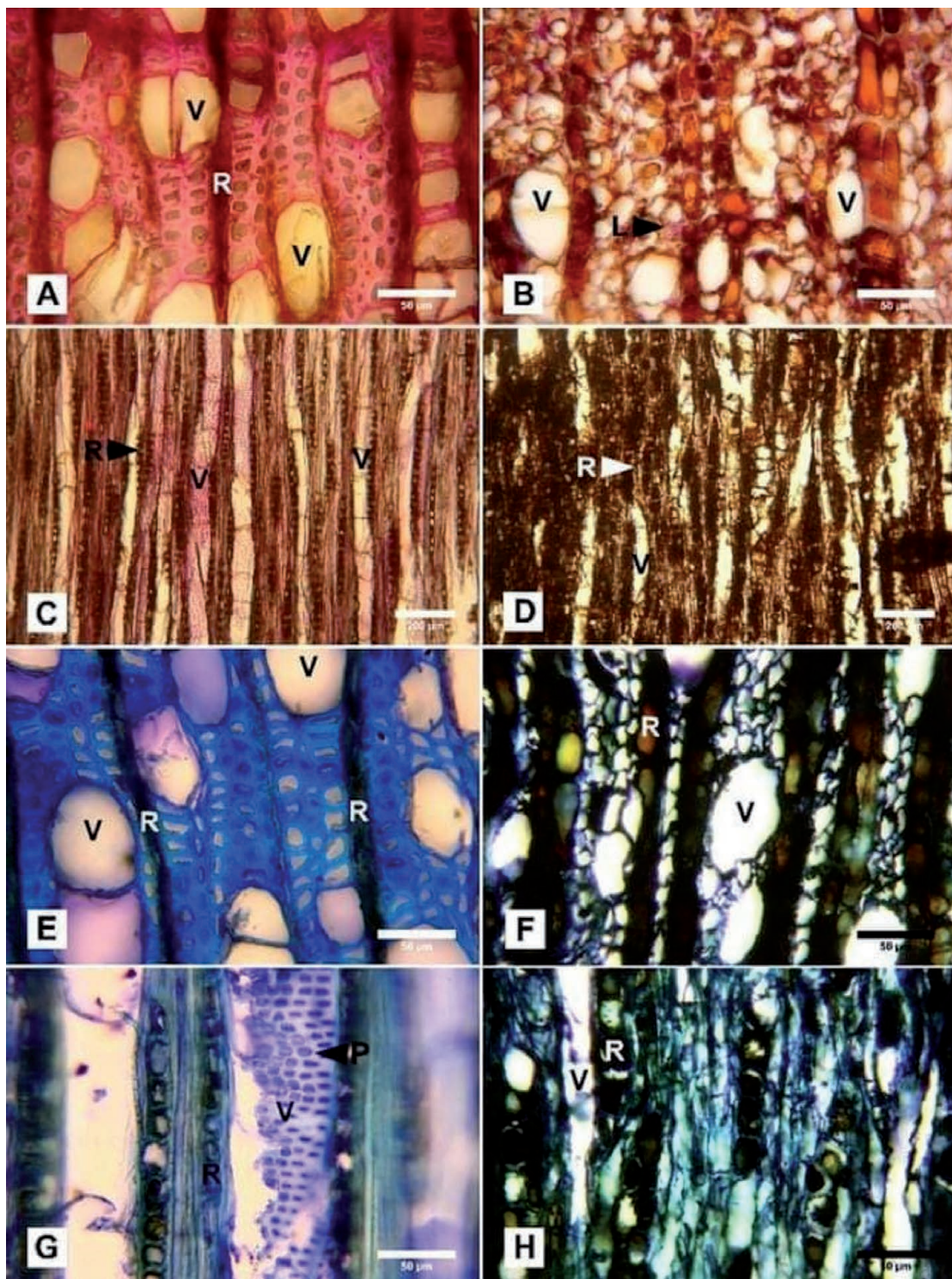


Fig. 2. Histochemistry of *Nothofagus dombeyi* uninfected wood (A, C, E, G) and infected by *C. olivacea* (B, D, F, H). A-D) stained with phloroglucinol. A) Cross-section with fibers and rays showing a positive reaction (pink) to lignin. B) Thin, degraded walls without pink coloration (negative reaction to lignin) and rays with large cells and reddish-brown contents. Only a few fibers with lignin contents (L) are observed. C) Tangential longitudinal section of the vessel walls and fibers showing the presence of lignin. D) Negative reaction for lignin indicating the action of the wood decay fungi. E-H) Detail of the cross-section stained with toluidine blue, where: E: the fibers and rays with dark contents are observed along with some pink vessels indicating the presence of carbohydrates. F) Thin, deformed and dark-colored walls. Other rays with dark contents deformed (enlarged) cells and translucent vessels due to the degradation of carbohydrates. G) Tangential longitudinal section of

- non-infected wood where fibers and intervacular pits appear stained in blue, indicating the presence of lignin. The rays show a greenish coloration (a weaker reaction for lignin) with darker deposits. H) Infected wood with the dark fibers of thin walls and rays showing enlarged cells of dark cellular contents. (L) = lignin; (V) = vessels; (R) = rays; (P) = intervacular pits.

Fig. 2. Histoquímica de madera no infectada de *Nothofagus dombeyi* (A, C, E, G) e infectada por *C. olivacea* (B, D, F, H) teñidas con floroglucinol. A) Sección transversal con fibras y radios mostrando reacción positiva (rosa) a lignina. B) Paredes delgadas, degradadas, sin coloración rosa (negativo para lignina) y radios de células grandes con contenidos castaño-rojizos. Solo se observan unas pocas fibras con contenido de lignina (L). C) Sección longitudinal de las fibras y paredes de los vasos mostrando presencia de lignina. D) Reacción negativa a la lignina indicando la acción de hongos degradadores. E-H) Detalle de secciones transversales teñidas con azul de toluidina en las que, E: se observan fibras y radios con contenidos oscuros se observan junto con algunos vasos en rosa que indica presencia de carbohidratos. G) Sección longitudinal tangencial de madera no infectada donde las fibras y las punteaduras intervacuolares aparecen teñidas de azul debido a la presencia de lignina. Los vasos muestran coloración verdosa (una reacción más débil a la lignina) con depósitos oscuros. H) Madera infectada con las fibras de paredes delgadas junto con radios que muestran células de contenido celular oscuro.

al precipitation) and Bio1 (annual mean temperature) contributing together with 81.6% (Table S3). Regarding the permutation importance, determined by random permutations of the values of each variable among the training points and background data, Bio12 and Bio1 also had the maximum influence on the model and contributed 82.6% (Table S3). The result of the jackknife test showed Bio1 has the most useful information by itself and the most information that is not present in other variables (Table S4). In general, suitability was high in areas with an annual mean temperature (Bio1) between 0 °C and 10 °C, and precipitation values (Bio12) in the range of 500-1,500 mm³ (Fig. 4). The potential distribution extends in areas with low-temperature variation throughout the day (Bio2), and low-temperature change over the course of the year (Bio4) (Fig. S2); and in areas where the coldest temperatures are between -10 °C and 0 °C (Bio11) and low precipitation seasonality (Bio15) (Fig. S4). The most suitable areas are found below 1,000 m.a.s.l. with a mean annual temperature of around 10 °C (Fig. S5).

DISCUSSION

The highest habitat suitability (> 0.8) for *C. olivacea* seems be limited to humid forests in latitudes higher than 35° on the Chilean slope of the Andes. On the Argentinean slope, areas of high suitability are more restricted, and limited to humid valleys in the provinces of Chubut, Santa Cruz and Tierra del Fuego. The rain seasonality seems to be decisive, slightly lowering the habitat suitability in the rest of the Andean Patagonia. This variable has shown to be also very influential, explaining the distribution of agaricoid fungal species in this region (Romano *et al.*, 2017). However, the whole Andean Patagonia displays an also alarming suitability value above 0.6, in a region with widespread use of wood as main construction material and where wood production is one of the most important economic activities.

This high suitability supports the recognition of this record as an alien species. The chances of this species staying unnoticed despite the huge sampling efforts in the last decades are very low; especially considering the intensive campaigns looking

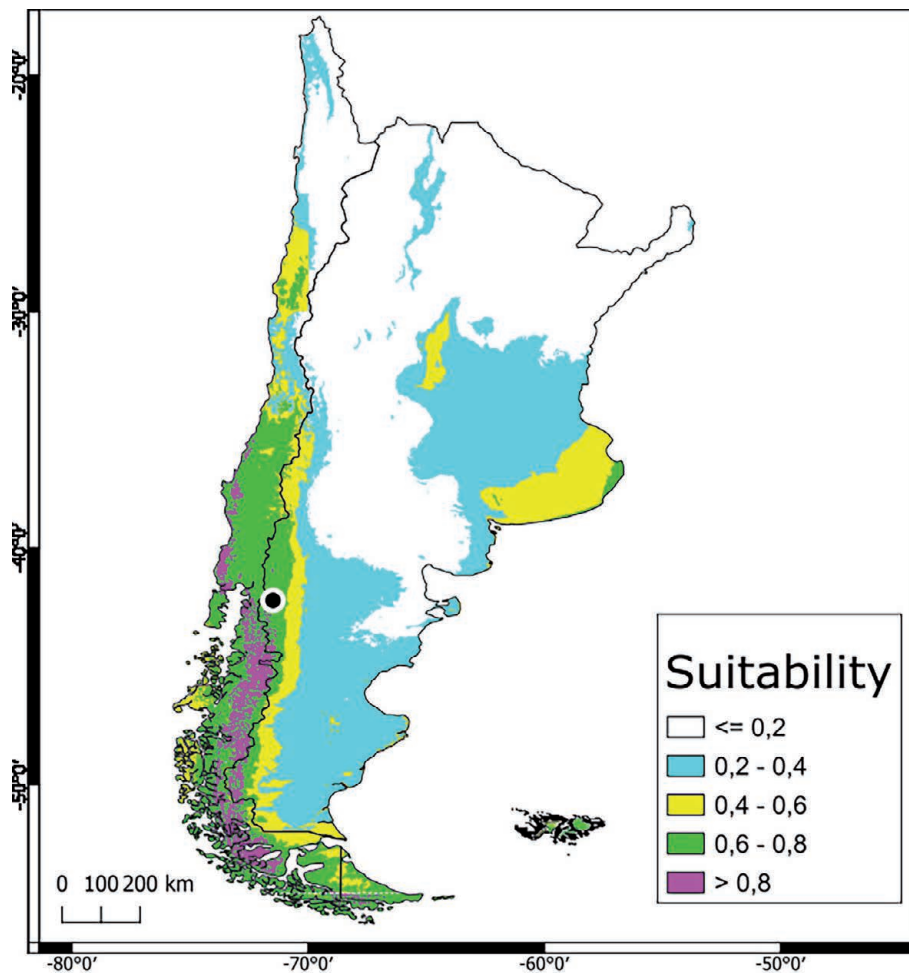


Fig. 3. Distribution of suitable habitat of *C. olivacea* in Argentina and Chile. The suitability value represents the predicted distribution probability (in logistic value) for climatic and elevation layers used in the niche modeling. Specimen of *C. olivacea* collected in Patagonia marked with a black dot.

Fig. 3. Distribución de hábitat idóneo para *C. olivacea* en Argentina y Chile. Los valores de idoneidad representan la distribución de probabilidad predicha (en valores logísticos) para las capas climáticas y de elevación usadas en el modelado de nicho. El espécimen de *C. olivacea* colectado en Patagonia se marca con un punto negro.

for corticioid fungi in this region (Gallo *et al.*, 2021). Also, the fact that the location of the collection studied has a long history of forestry and forest management speaks for a recent introduction.

An important subject to discuss here is the potential role of *C. olivacea* as a wood pathogen. There are some articles showing its role as a “butt rotter” in temperate and cold forests (Worrall & Nakasone, 2009) and also as a branch and stem rotter (Aref’ev, 1991). Although it is too early to suggest that this species might act as a pathogen in Patagonia, the fact that the Patagonian collection is associated with a native tree species, together with the high habitat suitability shown, indicates that this possibility should be considered. Evidence of delignification was found in the substrate of the studied voucher despite the fact that *C. olivacea* is a brown rot species. This suggests that attack by *C. olivaceae* may be a secondary colonization on a previously decayed material. Assays in living trees under controlled conditions

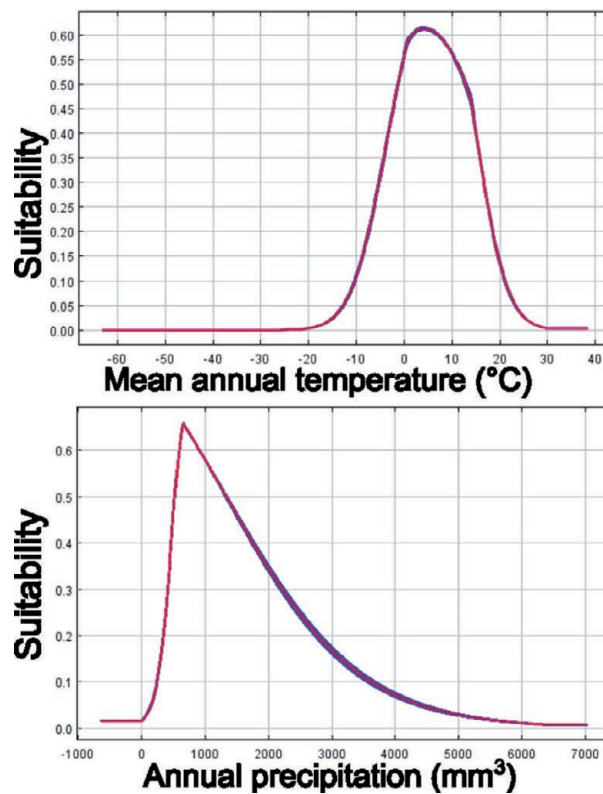


Fig. 4. Response curves of the most important environmental variables in modeling habitat distribution for *C. Olivacea*. Mean annual temperature (Bio1) and Annual precipitation (Bio12). The suitability value represents the predicted distribution probability on a logistic scale.

Fig. 4. Curvas de respuesta de las variables más importantes en el modelado de distribución de hábitat para *C. olivacea*. Temperatura anual media (Bio1) y precipitación anual (Bio12). El valor de idoneidad representa la distribución de probabilidad predicha en escala logística.

would be a potential way of assessing the latter. Furthermore, a more intense inspection of living trees in the areas surrounding the original location would provide invaluable information on this matter. The verification of potential pathogenicity on native trees would require immediate actions restricting the spread of this decayer, given the wide range of wood species where it can grow (Da Costa *et al.*, 1961).

Finally, genotyping of more collections would allow analyses that take into account the intraspecific diversity proposed by Kauserud *et al.* (2007). Such analyses are currently unviable given the number of registers needed to perform a supported prediction of the distributional range.

ACKNOWLEDGEMENTS

This work was supported by FONCyT (Grant PICT 2018 – 3781 to F.K.) and CONICET. The authors also thank Alejandro Bringas (CORD Herbarium), and the University of Patagonia San Juan Bosco (Esquel, Argentina) for their assistance. A special acknowledgment goes to Alina Greslebin, Andrés de Errasti, and Gabriela Gonzalez for proofreading early versions of the manuscript.

CONFLICT OF INTEREST

The authors declare that they have no conflict of interest.

REFERENCES

- Aref'ev, S. P. (1991). Xylotrophic fungi—the causal agents of Siberian pine (*Pinus sibirica* Du Tour) rot in the central taiga region of the Irtysh river basin. *Mikologiya i Fitopatologiya* 25 (5): 419-425.
- Chee, A. A., Farrell, R. L., Stewart, A. & Hill, R. A. (1998). Decay potential of basidiomycete fungi from *Pinus radiata*. *Proceedings of the New Zealand Plant Protection Conference* 51: 235-240. <https://doi.org/10.30843/nzpp.1998.51.11659>
- Da Costa, E. W. B., Rudman, P. & Gay, F. J. (1961). Relationship of growth rate and related factors to durability in *Tectona grandis*. *Empire Forestry Review* 40 n° 4 (106): 308-319.
- Da Costa, E. W. B. & Osborne, L. D. (1967). Comparative decay resistance of twenty-six New Guinea timber species in accelerated laboratory tests. *The Commonwealth Forestry Review* 46 (1): 63-74. <http://www.jstor.org/stable/42604717>
- Darriba, D., Taboada, G. L., Doallo, R. & Posada, D. (2012). jModel-Test 2: more models, new heuristics and parallel computing. *Nat Methods* 9: 772-772. <https://doi.org/10.1038/nmeth.2109>
- Desprez-Loustau, M. L., Robin, C., Buee, M., Courtecuisse, R., Garbaye, J., Suffert, F. & Rizzo, D. M. (2007). The fungal dimension of biological invasions. *Trends in Ecology & Evolution* 22 (9): 472-480. <https://doi.org/10.1016/j.tree.2007.04.005>
- Dickie, I. A., Bufford, J. L., Cobb, R. C., Desprez-Loustau, M. L., Grelet, G., Hulme, P. E., Klironomos, J., Makiola, A., Nuñez, M. A., Pringle, A. & Thrall, P. H. (2017). The emerging science of linked plant–fungal invasions. *New Phytologist* 215 (4): 1314-1332. <https://doi.org/10.1111/nph.14657>
- Edman, M. & Jonsson, B. G. (2001). Spatial pattern of downed logs and wood-decaying fungi in an old-growth *Picea abies* forest. *Journal of Vegetation Science* 12 (5): 609-620. <https://doi.org/10.2307/3236900>
- Elith, J. & Leathwick, J. R. (2009). Species Distribution Models: Ecological Explanation and Prediction Across Space and Time. *Annual Review of Ecology, Evolution, and Systematics* 40: 70-93. <https://doi.org/10.1146/annurev.ecolsys.110308.12015>
- Gallo, A. L., Silva, P. V., López Bernal, P., Moretto, A. S. & Greslebin, A. G. (2021). Fungal diversity, woody debris, and wood decomposition in managed and unmanaged Patagonian *Nothofagus pumilio* forests. *Mycological Progress* 20: 1309-1321. <https://doi.org/10.1007/s11557-021-01734-4>
- Gardes, M. & Bruns, T. D. (1993). ITS primers with enhanced specificity for basidiomycetes—application to the identification of mycorrhizae and rusts. *Molecular Ecology* 2: 113-118. <https://doi.org/10.1111/j.1365-294X.1993.tb00005.x>
- Ginns, J. (1982). A monograph of the genus *Coniophora* Aphyllophorales, Basidiomycetes. *Opera Botanica* 61: 1-61.
- Giordana, G., Kitzberger, T. & La Manna, L. (2020). Anthropogenic factors control the distribution of a southern conifer *Phytophthora* disease in a peri-urban area

- of northern Patagonia, Argentina. *Forests* 11 (1183): 1-17. <https://doi.org/10.3390/f11111183>
- Greslebin, A. G. & Rajchenberg, M. (2003). Diversity of Corticiaceae sens. lat. in Patagonia, southern Argentina. *New Zealand Journal of Botany* 41 (3): 437-446. <https://doi.org/10.1080/0028825X.2003.9512861>
- Guindon, S. Dufayard, J. F., Lefort, V., Anisimova, M., Hordijk, W. & Gascuel, O. (2010). New algorithms and methods to estimate maximum-likelihood phylogenies: assessing the performance of PhyML 3.0. *Systematic biology* 59 (3): 307-321. <https://doi.org/10.1093/sysbio/syq010>
- Hijmans, R. J., Cameron, S. E., Parra, J. L., Jones, P. G. & Jarvis, A. (2005). Very high resolution interpolated climate surfaces for global land areas. *International Journal of Climatology* 25: 1965-1978. <https://doi.org/10.1002/joc.1276>
- Huelsenbeck, J. P. & Ronquist, F. (2001). MrBayes: Bayesian inference of phylogenetic trees. *Bioinformatics* 17: 754-755. <https://doi.org/10.1093/bioinformatics/17.8.754>
- Kass, J. M., Vilela, B., Aiello-Lammens, M. E., Muscarella, R., Merow, C. & Anderson, R. P. (2018). Wallace: A flexible platform for reproducible modeling of species niches and distributions built for community expansion. *Methods in Ecology and Evolution* 9: 1151-1156. <https://doi.org/10.1111/2041-210X.12945>
- Katoh, K. & Standley, D. M. (2013). MAFFT multiple sequence alignment software 7: improvements in performance and usability. *Molecular Biology and Evolution* 30: 772-780. <https://doi.org/10.1093/molbev/mst010>
- Kauserud, H., Shalchian-Tabrizi, K. & Decock, C. (2007). Multilocus sequencing reveals multiple geographically structured lineages of *Coniophora arida* and *C. olivacea* (Boletales) in North America. *Mycologia* 99 (5): 705-713. <https://doi.org/10.3852/mycologia.99.5.705>
- Krishnamurthy, K. V. (Eds.) (1988). *Methods in Plant Histochemistry*. Madras: Viswanathan and Co.
- Peterson, A. T., Papes, M. & Soberon, J. (2008). Rethinking receiver operating characteristic analysis applications in ecological niche modeling. *Ecological Modelling* 213: 63-72. <https://doi.org/10.1016/j.ecolmodel.2007.11.008>
- Phillips, S. J., Anderson, R. P. & Schapire, R. E. (2006). Maximum entropy modeling of species geographic distributions. *Ecological Modelling* 190 (3-4): 231-259. <https://doi.org/10.1016/j.ecolmodel.2005.03.026>
- Phillips, S. J., Dudík, M. & Schapire, R. E. (2017). Maxent Software for Modeling Species Niches and Distributions [Software]. Version 3.4.0. [accessed 2023 Feb 28]. http://biodiversityinformatics.amnh.org/open_source/maxent/
- Rivera, S. M. (1988). Revisión xilológica del género *Nothofagus* Bl. (Fagaceae) para la Argentina. Buenos Aires: Monografías de la Academia Nacional de Ciencias Exactas, Físicas y Naturales. Vol. 4. p. 73-84.
- Rivera Nava, L., Quintanar, I. & Perez Olvera, C. (1999). Comparación histoquímica de albura y duramen de tres especies de *Quercus*. *Madera y Bosques* 5 (1): 27-41. <https://doi.org/10.21829/myb.1999.511352>

- Romano, G. M., Greslebin, A. G. & Lechner, B. E. (2017). Modelling agaricoid fungi distribution in Andean forests of Patagonia. *Nova Hedwigia* 105 (1-2): 95-120. https://doi.org/10.1127/nova_hedwigia/2016/0377
- Rudman, P. (1963). The Causes of Natural Durability in Timber-Pt. XII. The Deterioration in Antifungal Activity of Heartwood Extractives During the Life of Trees of *Eucalyptus marginata* Sm. *Holzforschung* 17 (3): 86-89. <https://doi.org/10.1515/hfsg.1963.17.3.86>
- Silva, P. V., Vélez, M. L., Hernández Otaño, D., Nuñez, C. & Greslebin, A. G. (2016). Action of fosetyl-al and metalaxyl against *Phytophthora austrocedri*. *Forest Pathology* 46 (1): 54-66. <https://doi.org/10.1111/efp.12216>
- Stalpers, J. (1978). Identification of wood-inhabiting fungi in pure culture. *Studies in Mycology* 16: 1-248.
- Tortorelli, L. A. (Eds.) (2009). *Maderas y bosques argentinos: tomo 1 (No. F50-01)*. Buenos Aires: Acmé.
- White, T. J., Bruns, T., Lee, S. & Taylor, J. (1990). *Amplification and direct sequencing of fungal ribosomal RNA genes for phylogenetics*, ed. Michael A. Innis, David H. Gelfand, John J. Sninsky, Thomas J. White, PCR Protocols, Academic Press, pp. 315-322, ISBN 9780123721808. <https://doi.org/10.1016/B978-0-12-372180-8.50042-1>
- Worrall, J. J. & Nakasone, K. K. (2009). Decays of Engelmann spruce and subalpine fir in the Rocky Mountains. USDA Forest Service Forest Insect and Disease Leaflet 150. In: U.S. Department of Agriculture, Forest Service, Pacific Northwest Region.
- Yuan, H. S, Wei, Y. L. & Wang, X. G. (2015). Maxent modeling for predicting the potential distribution of Sanghuang, an important group of medicinal fungi in China. *Fungal Ecology* 17: 140-145. <https://doi.org/10.1016/j.funeco.2015.06.001>

SUPPLEMENTARY MATERIAL

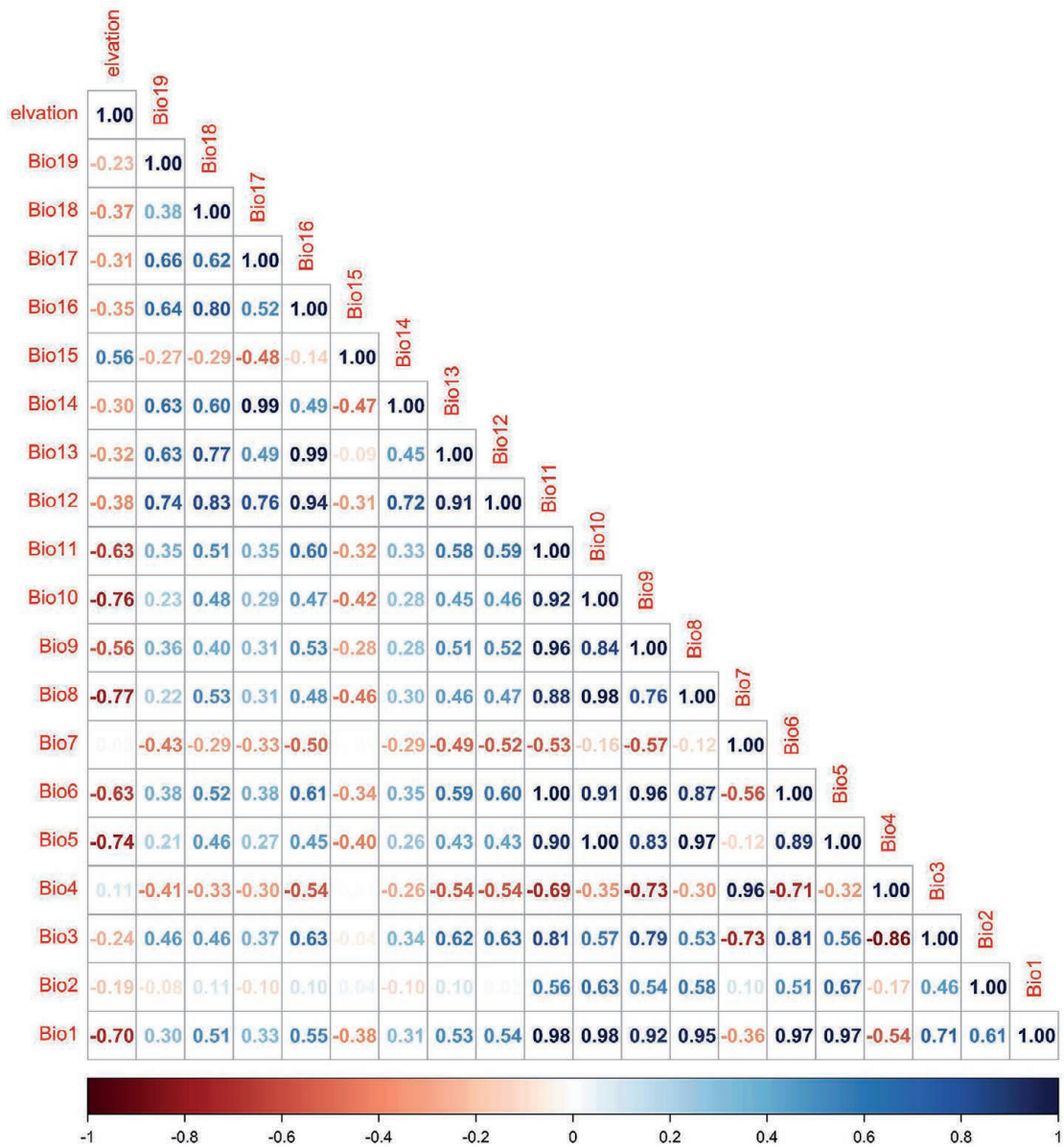


Fig. S1. Covariance matrix of bioclimatic and elevation layers calculated using Pearson’s correlation coefficient.

Fig. S1. Matriz de covarianza de las capas bioclimáticas y de elevación calculadas usando el coeficiente de correlación de Pearson.

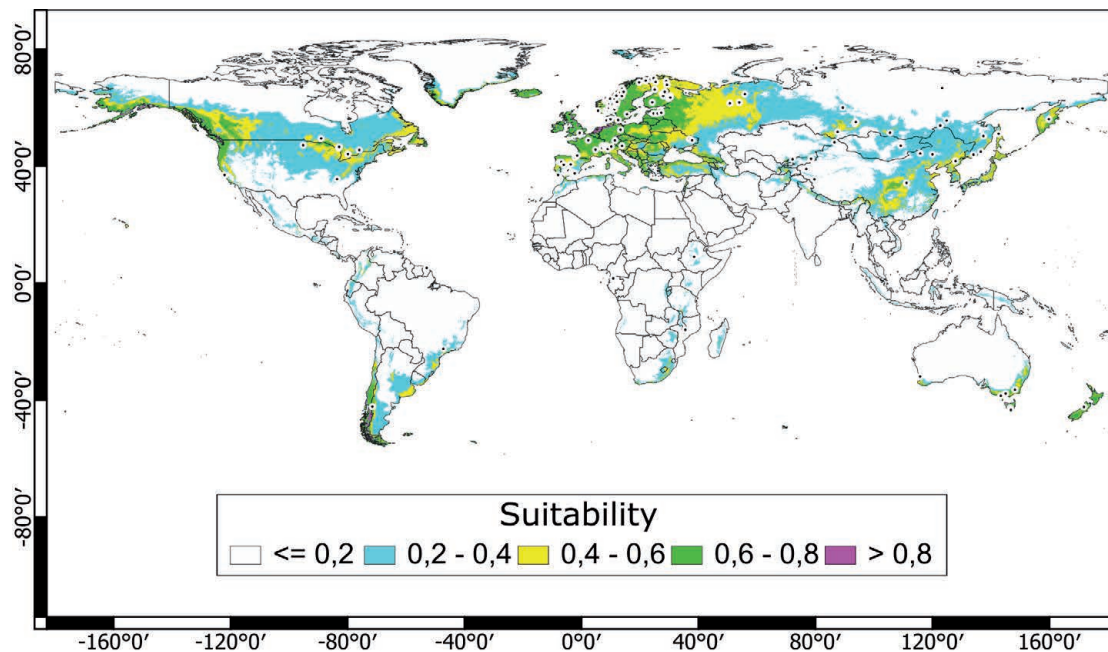


Fig. S2. Distribution of suitable habitat of *C. olivacea* worldwide. The suitability value represents the predicted distribution probability (in logistic value) for climatic and elevation layers used in the niche modeling. Specimens of *C. olivacea* are marked with a black dot.

Fig. S2. Distribución mundial de hábitat idóneo para *C. olivacea*. El valor de idoneidad representa la distribución de probabilidad predicha (en valor logístico) para las capas climáticas y de elevación.

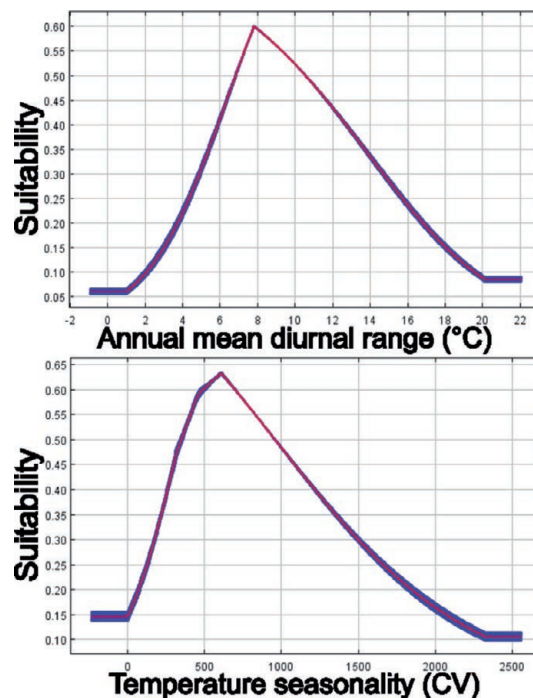


Fig. S3. Response curves of annual mean diurnal range (Bio2) and temperature seasonality (Bio4) in modeling habitat distribution for *C. olivacea*. The suitability value represents the predicted distribution probability (in logistic value).

Fig. S3. Curvas de respuesta de media anual de rango diurno (Bio2) y estacionalidad de la temperatura (Bio4) en el modelado de distribución de hábitat para *C. olivacea*. El valor de idoneidad representa la distribución de probabilidad (en escala logística).

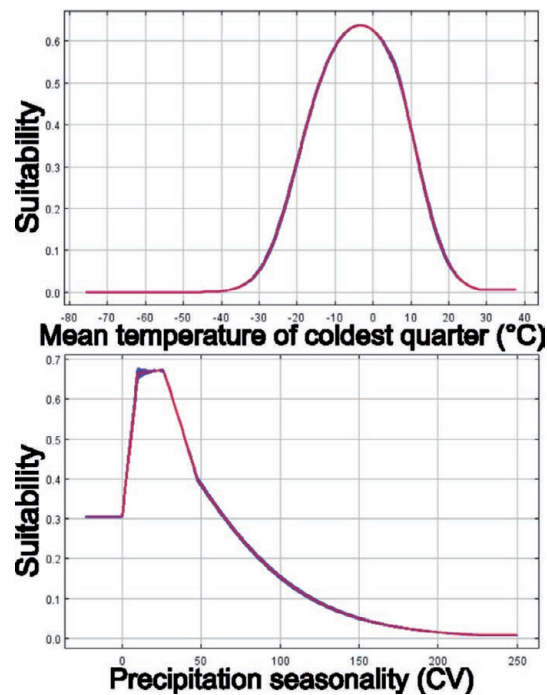


Fig. S4. Response curves of the mean temperature of the coldest quarter (Bio11) and precipitation seasonality (Bio15) in modeling habitat distribution for *C. olivacea*. The suitability value represents the predicted distribution probability (in logistic value).

Fig. S4. Curvas de respuesta de la temperatura media del trimestre más frío (Bio11) y estacionalidad de la precipitación (Bio15) al modelar la distribución de hábitat de *C. olivacea*. El valor de idoneidad representa la distribución de probabilidad predicha (en escala logística).

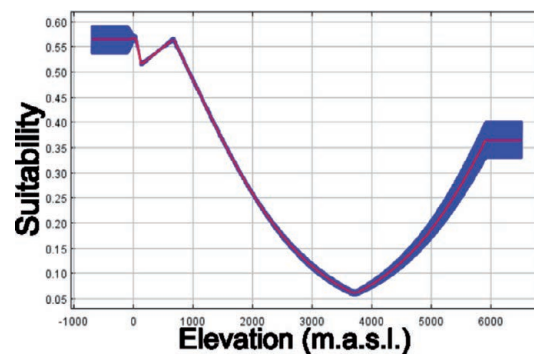


Fig. S5. Response curve of the elevation layer in modeling habitat distribution for *C. olivacea*. The suitability value represents the predicted distribution probability (in logistic value).

Fig. S5. Curva de respuesta de la capa de elevación al modelar la distribución de hábitat de *C. olivacea*. The suitability value represents the predicted distribution probability (in logistic value).

Table S1. GenBank Accession numbers of the sequences used in the tree, voucher numbers, and country of origin.

Tabla S1. Números de identificación de GenBank de las secuencias utilizadas en el árbol, números de ejemplar de fungario, y país de origen.

GenBank	Species	Voucher	Origin
AJ518879	<i>Coniophora marmorata</i>	P158	Germany
AM747518	<i>Coniophora olivacea</i>	MUCL 20566	Germany
AM747520	<i>Coniophora olivacea</i>	82/34/3	Norway
AM747523	<i>Coniophora olivacea</i>	FP100334	USA
AM747529	<i>Coniophora olivacea</i>	DAOM 216045	Canada
AM747530	<i>Coniophora olivacea</i>	FPL1	UK
AM747533	<i>Coniophora olivacea</i>	MD204	USA
AM946632	<i>Coniophora marmorata</i>	FPRL 410	UK
AM747527	<i>Coniophora olivacea</i>	FP105383	USA
ON832657	<i>Coniophora olivacea</i>	FK16004	Argentina
DQ202271	<i>Coniophora arida</i>	AFTOL-ID 698	USA
FJ790314	<i>Coniophora opuntiae</i>	AH31855	Spain
GU187516	<i>Coniophora olivacea</i>	FP104386	USA
GU187527	<i>Leucogyrophana arizonica</i>	RLG-9902	USA
GU187532	<i>Leucogyrophana olivascens</i>	HHB-11134	USA
HF921467	<i>Coniophora fusispora</i>	15702Tell	Spain
HG326617	<i>Coniophora eremophila</i>	19021Tell	Spain
HG326618	<i>Coniophora eremophila</i>	MAFungi 86372	Cape Verde
MG763873	<i>Coniophora hanoiensis</i>	He5197	Vietnam
MG763874	<i>Coniophora hanoiensis</i>	He5202	Vietnam
MG763875	<i>Coniophora arida</i>	He4658	Vietnam
MW192497	<i>Coniophora sp.</i>	He6920	Vietnam
MW192498	<i>Coniophora sp.</i>	He6926	Vietnam
OL898499	<i>Coniophora olivacea</i>	MUCL 20566	Germany
OM972325	<i>Leucogyrophana olivascens</i>	S.D.Russell 54	USA
GU066829	<i>Coniophora puteana</i>	LMSA1.03.047	France
JQ765680	<i>Coniophora puteana</i>	ISOL01	Sweden

Table S2 (1 of 2). Source, coordinates, and identity of the specialist who determined the specimen of locations used in niche modeling of *C. olivacea*.**Tabla S2 (1 de 2).** Fuente, coordenadas e identidad del especialista que determinó los especímenes de las locaciones usadas en el modelado de nicho de *C. olivacea*.

Source	Identifier	Identified by	Latitude	Longitude
GBIF	2853840061	N. Nguyen	-43.3667	-122.0550
GBIF	2853817742	Leif Ryvarde	-42.6833	-95.1651
GBIF	1803055872	Larsen, J.M.	-42.3250	-89.0226
GBIF	2468717113	Leif Ryvarde	-37.8167	-83.5569
GBIF	2872775370	Weresub, L.K.	-37.5167	-83.0383
GBIF	1929804531	Cain, R.F.	-36.4931	-82.8524
GBIF	78480752	Weresub, L.K.	-36.4800	-79.8667
GBIF	78480725	Weresub, L.K.	-33.3650	-75.9713
GBIF	3110699572	G. Gruhn	-31.9610	-52.9281
GBIF	31921821	Penteado, VL	-31.9610	-47.2314
GBIF	78480990	M.T.Telleria	-22.4872	-7.9800
GBIF	3128717799	M.T.Telleria	-15.9754	-7.5600
GBIF	1046448598	M.T.Telleria	8.9713	-6.8700
GBIF	1046448588	S. Pérez Gorjón	30.2496	-6.0500
GBIF	1046448584	N. Rodríguez Ramos	37.0300	-5.7000
GBIF	78480692	Pérez-Daniëls, P.	37.5900	-4.8209
GBIF	78480750	De Esteban J.	37.7573	-4.4358
GBIF	78480751	M.Dueñas	37.9300	-3.6800
GBIF	2640619325	Guerra, A.	37.9700	-3.4882
GBIF	2640611323	M.T.Telleria	38.5045	-2.8500
GBIF	3128711770	K.Hjortstam	40.4400	-2.2900
GBIF	3128712088	Riezu J.M.	40.4400	-2.1423
GBIF	3022691275	Martin J.	40.4400	-1.4509
GBIF	1412705076	Leif Ryvarde	40.5900	-0.6089
GBIF	3120315712	Melo & Salcedo	41.3400	4.8144
GBIF	3119888857	Leif Ryvarde	41.4100	5.6849
GBIF	3119941694	Jean Keller	41.7449	7.0766
GBIF	3120085534	Keller Jean	41.7449	7.0820
GBIF	3120083547	Mykologische Gesellschaft Luzern	42.8330	8.0603
GBIF	1935675408	Tom Helliik Hofton	43.0205	8.1391
GBIF	2580067375	Even Høgholen	43.9667	8.2132
GBIF	1935674992	Finn Oldervik	45.5582	8.3158
GBIF	2640622329	Kilian Mühlebach	45.8390	8.4596
GBIF	1935675508	Gian-Felice Lucchini	45.8390	8.5111
GBIF	2464714773	Thomas Læssøe	46.1528	8.6163
GBIF	2464715470	Geir Gaarder, B. Bredesen	46.3825	8.9995
GBIF	2464715186	Eleno Zenone	46.3838	9.0153
GBIF	3022675674	Geir Gaarder	46.9750	9.1313
GBIF	3022678099	Leif Ryvarde	47.0853	9.3892
GBIF	3022678092	Even Høgholen	47.1264	9.4323
GBIF	125721900	Even W. Hanssen	47.1948	9.4771
GBIF	3022691280	Gaute Mohn Jenssen	47.3250	9.6800
GBIF	3022711521	Egil Bendiksen, Klaus Høgholen	49.0760	9.8276
GBIF	3022710706	Jan Vesterholt	49.0760	9.9203
GBIF	3022660912	Baici & Horak	49.0760	10.2184
GBIF	3022670965	Leif Ryvarde	51.1364	10.5434
GBIF	2332466434	Egil Bendiksen, Klaus Høgholen	54.6592	10.6756
GBIF	2592349870	Leif Ryvarde	54.6592	10.6958
GBIF	2332386590	Hofton, Tom H.	56.0200	11.3122
GBIF	2332484109	Viacheslav Spirin	56.0477	11.3900
GBIF	3022678738	L. Ryvarde	57.8083	11.6876
GBIF	2332380451	Leif Ryvarde	58.0167	11.9530
GBIF	2332484110	Leif Ryvarde	58.2670	12.0205
GBIF	2332499532	Halvor Solheim	58.2808	12.1902
GBIF	3022677158	Thomas Læssøe	59.0407	12.5515
GBIF	2332484140	Leif Ryvarde	59.5106	13.2995
GBIF	2332329295	Leif Ryvarde	59.6542	13.8343

Table S2 (2 of 2). Source, coordinates, and identity of the specialist who determined the specimen of locations used in niche modeling of *C. olivacea*.

Tabla S2 (2 de 2). Fuente, coordenadas e identidad del especialista que determinó los especímenes de las locaciones usadas en el modelado de nicho de *C. olivacea*.

Source	Identifier	Identified by	Latitude	Longitude
GBIF	2332330958	Michelitsch Siegmund	59.6696	13.8917
GBIF	2332484094	L. Ryvarden	59.7348	13.9566
GBIF	2332484137	L. Ryvarden	59.9492	14.4268
GBIF	2332484088	Gro Gulden, J. Eriksson	60.1817	15.5935
GBIF	2332484086	Gunnar Kristiansen	60.1879	19.7542
GBIF	2332328417	Leif Ryvarden	60.2405	21.9905
GBIF	2332484099	Leif Ryvarden	60.5576	23.7227
GBIF	2332484100	K. Juutilainen	60.6690	24.2320
GBIF	2332484097	Erast Parmasto	60.7622	24.7000
GBIF	3022710206	Leif Ryvarden	60.7711	24.7060
GBIF	2332471091	Kulju, Matti	60.8157	25.0803
GBIF	2332484085	Leif Ryvarden	60.9684	25.3705
GBIF	1052045733	Erast Parmasto	61.1078	26.0733
GBIF	2332381834	Erast Parmasto	61.1969	27.0167
GBIF	2332382904	Erast Parmasto	61.2661	27.3217
GBIF	2332382048	Moilanen, Aki	61.2885	27.6367
GBIF	2332484089	Kulju, Matti	61.3041	27.9667
GBIF	3460838722	Kulju, Matti	61.5546	28.4940
GBIF	2332444819	Leif Ryvarden	61.5841	28.9949
GBIF	773226377	Kulju, Matti	61.6537	29.2642
GBIF	3460843518	E.Parmasto	61.7167	29.7911
GBIF	2332399347	Lehtonen Hannu	61.7291	30.3716
GBIF	3441197293	M. Kirsi	61.7413	30.4114
GBIF	2332460790	Viacheslav Spirin scr.	61.7453	35.5262
GBIF	2991518006	Alexander Ordynets	61.7694	36.9845
GBIF	2332445204	Alexander Ordynets	63.0420	37.8528
GBIF	3441185087	Leif Ryvarden	63.0432	38.5651
GBIF	3022706988	Erast Parmasto	63.0842	50.7887
GBIF	3022660067	Erast Parmasto	63.1253	53.9975
GBIF	3713361932	Ain Raitviir	63.2220	55.9065
GBIF	3107784828	Erast Parmasto	63.9944	78.5390
GBIF	2332329461	Erast Parmasto	64.0315	80.3301
GBIF	3713366539	Erast Parmasto	64.1358	87.6215
GBIF	3022678766	Erast Parmasto	64.2939	89.3966
GBIF	3713359652	Erast Parmasto	64.6526	93.4100
GBIF	3107787449	Erast Parmasto	64.6922	93.8500
GBIF	3460839026	N.L. Bougher	64.6922	115.8229
GBIF	2569344336	Erast Parmasto	64.7388	123.3742
GBIF	2332484113	Erast Parmasto	65.2961	124.9180
GBIF	2332484108	Leif Ryvarden	65.4551	127.9663
GBIF	1324376586	Erast Parmasto	66.3129	134.0667
GBIF	2332458095	Erast Parmasto	66.7660	136.5833
GBIF	2332484111	Erast Parmasto	67.8899	137.5000
GBIF	3022678668	Erast Parmasto	68.7227	142.6847
GenBank	AJ344112	Olaf Schmidt et al., 2002	48.8569	2.3513
GenBank	ON832657	This Article	-42.2181	-71.4961
GenBank	AM747520	Kauserud, H. et al., 2007	1.635	10.8741
GenBank	AJ345009	Olaf Schmidt et al., 2002	48.8409	11.4395
GenBank	AM747519	Kauserud, H. et al., 2007	52.5166	13.3833
GenBank	AM747527	Kauserud, H. et al., 2007	42.38	72.2282
GenBank	GU187516	Binder, M. et al., 2010	39.0276	76.9039
GenBank	AM747528	Kauserud, H. et al., 2007	35.5481	79.6967
GenBank	AM747526	Kauserud, H. et al., 2007	47.0331	109.2266
GenBank	AM747537	Kauserud, H. et al., 2007	34.3131	111.1993
GenBank	AM747533	Kauserud, H. et al., 2007	44.0384	120.0599
GenBank	AM747531	Kauserud, H. et al., 2007	53.9218	122.7267

Table S3. Contribution of each environmental variable used to predict the potential geographic distribution of *C. olivacea*. The values shown represent the average of 100 replicates. Values in bold indicate higher percent contribution and permutation importance.

Tabla S3. Contribución de cada variable ambiental usada para predecir la potencial distribución geográfica de *C. olivacea*. Los valores mostrados representan la media de cien réplicas. Los valores en negrita se corresponden con los mayores porcentajes de contribución e importancia de permutación.

	Variable	<i>Coniophora olivacea</i>
n		100
AUC ± SD		0.91 ± 0.09
Percent Contribution (%)	Bio1	43.1
	Bio2	4.5
	Bio4	3.7
	Bio11	7.1
	Bio12	38.5
	Bio15	0.4
	Elv	2.7
Permutation importance (%)	Bio1	78.9
	Bio2	0.5
	Bio4	8.1
	Bio11	7
	Bio12	3.7
	Bio15	0.9
	Elv	2.8

Table S4. Jackknife of regularized training gain for *C. olivacea*. Variable Bio1 contains the most useful information. Without this variable, the gain value decreases dramatically.

Tabla S4. Entrenamiento regularizado de ganancia de jackknife para *C. olivacea*. La variable Bio1 contiene la información más relevante. Sin ella, el valor de ganancia disminuye dramáticamente.

Variable	With only variable	Without variable	With all variables
Bio1	0.99	1.29	1.37
Bio2	0.07	1.34	
Bio4	0.11	1.37	
Bio11	0.87	1.37	
Bio12	0.65	1.33	
Bio15	0.43	1.37	
Elv	0.14	1.33	